ACS APPLIED MATERIALS & INTERFACES

Research Article

www.acsami.org

Rapid and Ultrasensitive Electrochemical Detection of Multidrug-Resistant Bacteria Based on Nanostructured Gold Coated ITO Electrode

Xiayi Lv,[†,‡] Wei Ge,[†] Qiwei Li,[†] Yueli Wu,[†] Hui Jiang,[†] and Xuemei Wang*[,†]

[†]State Key Laboratory of Bioelectronics (Chien-Shiung Wu Laboratory), Department of Biological Science and Medical Engineering, Southeast University, Nanjing 210096, China

[‡]School of Chemistry and Chemical Engineering, Southeast University, Nanjing 211189, China

Supporting Information

ABSTRACT: Rapid and ultrasensitive detection of pathogenic bacteria and their relevant multidrug resistance is particularly important in clinical diagnosis, disease control, and environmental monitoring. In this contribution, we have explored the possibility to rapidly detect some important disease related bacteria based on a nanostructured Au modified indium tin oxide electrode through the antibiotic agents such as doxorubicin. The rapid and real-time electrochemical detection of multidrug resistant bacteria like *Escherichia coli* and *Staphylococcus aureus* could be readily realized through the nanostructured Au based biosensor with high sensitivity. The observations of surface-enhanced Raman spectroscopy and laser confocal fluorescence microscopy also demonstrate the effectiveness of the relevant new strategy for the rapid and ultrasensitive electrochemical detection of some disease related bacteria.

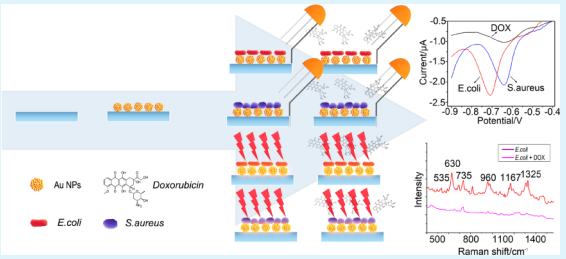

KEYWORDS: *electrochemical detection, surface enhanced Raman spectroscopy, doxorubicin, nanostructured Au modified ITO electrode*

1. INTRODUCTION

In the last decades, the incidence of resistance to antimicrobial agents of pathogens has been steadily rising, in food as well as in clinical isolates, which is associated with widely intensive use of antibiotics in livestock and in human health care.[1,2] Multidrug-resistant organisms (MDROs), such as methicillin-resistant *Staphylococcus aureus* (MRSA), vancomycin-resistant enterococci (VRE), and certain Gram-negative bacilli (GNB), are frequently resistant to most available antimicrobial agents.[3,4] On the basis of those observations, highly sensitive detection of pathogenic bacteria and their relevant drug resistance is particularly important in clinical diagnosis, disease control, environmental monitoring, and food safety. The traditional and common strategy of pathogen identification includes polymerase chain reaction (PCR),[5] culture and colony counting,[6] immunological techniques,[7] electrochemical analysis,[8−10] microarray detection, and fluorescence based assays using organic dye molecules,[11,12] with the detection limits in the range of 10^3 CFU mL^{-1}.

The growth of Gram-positive bacteria like *Staphylococcus aureus* and Gram-negative bacteria like *Escherichia coli* could be inhibited through the binding with anthracycline antibiotic agents such as doxorubicin (DOX), pharmorubicin, and daunorubicin. As a typical anthracycline antibiotic drug, DOX has been widely used in the treatment of several kinds of cancers, including severely lymphoblastic leukemia, gastric, and osteogenic sarcomas, breast, thyroid, genitourinary and bronchogenic carcinomas.[13−16] The DOX contains quinone and hydroquinone moieties that can be readily oxidized and reduced at various kinds of electrodes.[17] The interaction of microbes with antibiotic drugs like DOX has been investigated by various biochemical and physicochemical methods including molecule dynamics simulation,[18] electrical linear dichroism,[19] scanning electron microscopy (SEM),[20] and bioelectrochemical analysis.[21] Meanwhile, recent advances in the synthesis of biomolecular-functionalized nanomaterials have led to a wide range of applications of such assemblies in the generation of 2D and 3D ordered structures in solutions and on surfaces; particular application is directed to the use of biomolecule−nanoparticle (metallic or semiconductive) assemblies for bioanalytical applications and for the fabrication of bioelectronic devices.[22,23] On the basis of these observations, in this contribution, we have explored the possibility to utilize the DOX as a sensitive probe to recognize some disease related bacteria based on nanostructured a Au modified indium tin oxide (ITO) electrode. Moreover, by combining with the fluorescence as well as Raman spectroscopy,[24] it is interesting to note that the specific binding behavior of the anthracycline

Received: September 5, 2013
Accepted: June 20, 2014
Published: June 20, 2014

antibiotic drug with target bacteria could be readily observed, which could offer a convenient and sensitive way to monitor the molecular recognition and interaction process of relevant biological systems. Especially, the surface-enhanced Raman scattering (SERS) spectroscopy based on a nanostructured Au interface could specifically probe vibrations of the atoms within the molecule and hence bring additional evidence to physicochemical characterization of microorganisms,[25−27] i.e., identifying of bacteria cell components such as fatty acids, proteins, nucleic acids, and carbohydrates, from which the pathogenic bacteria could be rapidly and sensitively detected through the binding agent DOX on a nanostructured Au nanoparticles (NPs) modified electrode.

2. EXPERIMENTAL SECTION

2.1. Bacterial Strain and Culture Condition. Types of ATCC control strains (i.e., *Escherichia coli* ATCC 25922, *Staphylococcus aureus* ATCC 25923, *Acinetobacter baumannii* ATCC 94655) were purchased from American Type Culture Collection (ATCC). This strain was grown in tryptic soy broth (TSB) (Fluka, Buchs, Switzerland) or tryptic soy agar (TSA) (Fluka) plates for cell propagation. The number of colony-forming units (CFU) of the organisms was determined after quantitative culture on TSA plates. The batch of medium (pH 7.2) was inoculated from TSA plates containing freshly grown bacterial strains and incubated overnight in a thermostatic oscillator at 37 °C, shaking at 180 rpm.

2.2. Materials. DOX hydrochloride was obtained from Sigma-Aldrich and DOX (doxorubicin HCl liposome injection) was from Ortho Biotech Products. Solutions of different concentrations of doxorubicin were prepared in ultrapure water or PBS. ITO conductive glass (square resistance ≤40 Ω/cm^2) was obtained from Kangdake Applied Film Center (Jintan, China) and was cut into stripes of 3 × 0.5 cm, setting a fixed area of 0.25 cm^2 (0.5 × 0.5 cm) as the conducting surface of the electrode. Prior to electrochemical study, the ITO was ultrasonicated in acetone, ethanol, and water in turn for 5 min and thoroughly dried before following nanostructured Au NPs modification.

2.3. Preparation of Au NPs Modified Electrode. The nanostructured Au NPs were deposited onto the electrode by the multipotential step technique after washing the ITO. The depositing media were 0.5 M H_2SO_4 aqueous solution, containing 2.0 mM $HAuCl_4$ precursor and 25 μM cysteine, respectively. In this deposition process, the cysteine was added to the media to control the size of the nanostructured Au NPs and the potentials from 0 to 0.45 V (vs saturated calomel electrode, SCE) were applied to the system in turn. The running time, period, and dosage of cysteine were optimized to obtain the best conditions. After this process, the surfaces of the electrode were carefully washed and characterized. The peak current of differential pulse voltammetry (DPV) of $[Fe(CN)_6]^{3-/4-}$ increased accordingly on the Au NPs modified electrode, indicating the enhanced electron transfer on the nanostructured Au modified ITO electrode surface.

2.4. SEM and Raman Spectroscopic Study. The SEM images were obtained with an ULTRA PLUS field emission scanning electron microscope (Zeiss, Germany), with an acceleration potential at 10 kV. All experiments were performed at 25 ± 2 °C. Raman spectra were recorded with a confocal Raman microspectrometer (Renishaw Invia Reflex system) equipped with a Peltier-cooled charge-coupled device (CCD). The confocal microscope is coupled to a 460 mm focal length spectrograph equipped with a four interchangeable gratings turret. For Raman imaging, a drop of 10 μL cell suspension including *E. coli* or *S. aureus* is deposited onto the nanostructured Au modified electrode and placed in the incubator at 37 °C for 2 h. Afterward, a drop of 10 μL of DOX solution is added to the relevant nanointerface for cellular interaction study. An excitation wavelength at 785 nm, 50% laser intensity, and twice overlying with 100 s integration time was used to perform confocal Raman spectroscopy.

2.5. Electrochemical Detection. The electrochemical study including differential pulse voltammetry (DPV) and others was performed on a CHI660B electrochemical workstation (CH Incorporation, USA), using an ITO electrode as the working electrode, a Pt wire as the counter electrode, and a Ag wire as the reference electrode. The reference potential of the Ag wire was calibrated as a saturated calomel electrode (SCE), according to the relationship $V_{Ag} = V_{SCE} - 0.07$ V. The electrochemical impedance spectra (EIS) were carried out on an Autolab PGSTAT302N system (Eco Chemie, The Netherlands) using a conventional three-electrode system, i.e., an ITO electrode as the work electrode, a Pt wire as the counter, and a SCE as the reference electrode, respectively. Every experiment has been repeated at least three times.

2.6. Laser Confocal Fluorescence Microscopy (LCFM) Study. The LCFM images were obtained on a Carl Zeiss LSM710 (Zeiss, Germany), with an automatic inverted microscope Axio Observer.Z1. Before the imaging, the samples were successively immobilized with paraformaldehyde solution for 20 min and then dipped in 20 mM phosphate buffer solution (pH 7.4) three times for 15 min to remove dissociative bacteria either excessive or adsorptive probe molecules. A 488 nm excitation laser beam (Andor Revolution XD) was focused using a 20× IR coated objective (Nikon).

3. RESULTS AND DISCUSSION

3.1. Preparation and Characterization of the Nanostructured Au NPs Modified ITO Electrode. Initially, the nanostructured Au NPs modified ITO electrode was prepared through the procedure of multipotential step technique, as described previously. Then, a drop of 10 μL of cell suspension including *E. coli* or *S. aureus* is deposited onto the nanostructured Au modified electrode and placed in the incubator at 37 °C for 2 h. Afterward, a drop of 10 μL of DOX solution is added to the nanointerface of the nanostructured Au modified ITO electrode and detected through electrochemical study or Raman spectroscopy.

As shown in Figure 1A, the electrochemical study demonstrates that compared to the bare ITO electrode, the relevant peak current of $[Fe(CN)_6]^{3-/4-}$ on the nanostructured Au NPs modified ITO electrode increased remarkably, suggesting the apparently enhanced electron transfer on the Au NPs modified ITO electrode surface. Meanwhile, it is observed that the concentration of cysteine significantly affected the peak current on the nanostructured Au NPs modified ITO electrode, which displayed the good electrochemical behavior at the cysteine concentration of 25 μM. Besides, the series of the cyclic periods in the multipotential steps set with different period time also displayed different effects, where the period time of 1 s is the optimized cyclic period time (Figure 1B).

Moreover, the running time for the deposition process can also significantly affect the DPV signal, as shown in Figure 1C, which was chosen from 300 to 800 s with a fixed period of 1 s.

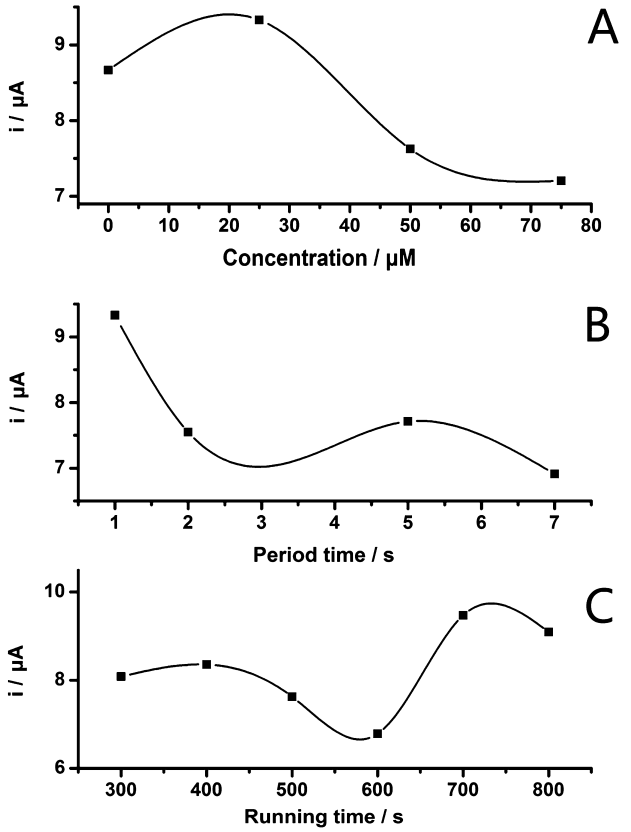

Figure 1. Effect of different factors on the DPV response of Au deposited ITO electrode in 10 mM $[Fe(CN)_6]^{3-}$ (containing 0.1 M KCl), including (A) the cysteine concentration; (B) the cyclic periods in the multipotential steps; (C) deposition time. The depositing media are 0.5 M H_2SO_4, 2.0 mM $HAuCl_4$, and 25 mM cysteine.

It is evident that the peak current of $[Fe(CN)_6]^{3-/4-}$ initially increased with the running time; however, with the running time up to 700 s, the peak current started to decrease. On the basis of the above observations, 700 s was chosen as the optimized deposition time with cyclic period time of 1 s.

The nanostructured surface morphology of the Au NPs modified ITO electrode could also have a significant effect on the sensitivity of electrochemical detection, which was further explored by SEM characterization. As shown in Figure 2, the SEM images of the nanostructured Au modified ITO electrodes illustrate the nice coverage of Au NPs on the surface of ITO electrodes with the formation of the nanoporous Au film (see Figure 3 for a schematic illustration for bacteria detection). The process of bacterial detection by using nanostructured Au based biosensor was shown in Figure 3. In the first step, the nanostructured Au modified ITO electrode was prepared by the multipotential step technique. Then, a drop of 10 μL of cell suspension including *E. coli* or *S. aureus* is deposited onto the nanostructured Au modified electrode and placed in the incubator at 37 °C for 2 h. Afterward, a drop of 10 μL of DOX solution is added to the nanointerface of the nanostructured Au modified ITO electrode and detected through electrochemical study or Raman spectroscopy. Due to the specific shape and nanoscaled structure of Au NPs, the relevant cells could readily interact with the nanostructured layer of the Au NPs modified electrodes to facilitate the attachment of bacteria. Meanwhile, it is noted that there is some apparent difference between the DOX treated cell morphology and the original bacteria cell

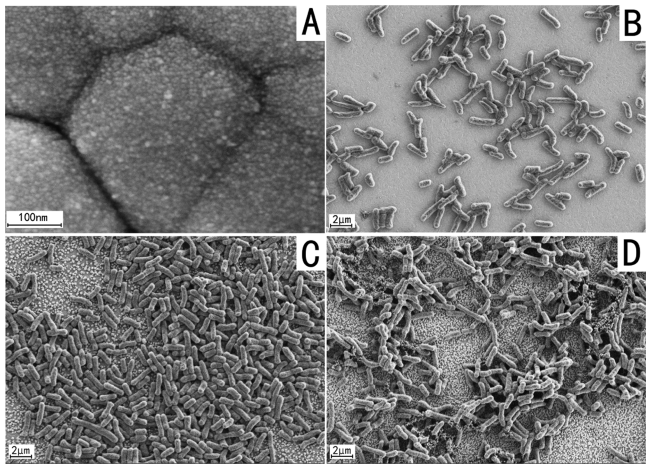

Figure 2. SEM images of (A) the nanostructured Au modified ITO electrodes, (B) *E. coli* cells on the surface of ITO, (C) *E. coli* cells on the nanostructured Au modified ITO electrodes, and (D) DOX treated *E. coli* cells on the nanostructured Au modified ITO electrodes.

morphology on relevant ITO electrodes (Figure 2C,D). This suggests the significant influence of DOX on the cell interaction and attachment, which could lead to the sensitively electrochemical detection of the relevant bacteria on the nanostructured Au NPs modified ITO electrodes (Figures 4B and S2 (Supporting Information)). Especially, our observations demonstrate that multidrug resistant bacteria like *E. coli* and *S. aureus* could be readily and rapidly distinguished based on the nano Au-coated biosensors.

3.2. Fluorescence (LCFM) and Surface Enhanced Raman Spectroscopic Study of the Cellular Interaction.

On the basis of the above study, laser confocal fluorescence microscopy (LCFM) and surface-enhanced Raman scattering (SERS) spectroscopy has been further utilized to explore the interaction process of relevant biological systems. As shown in Figure S1 (Supporting Information), the LCFM studies indicate that DOX could be readily endocytosed from extracellular matrix, which can considerably decrease the cell survival ratio through increasing the relevant incubation time. The effects of probe molecule DOX on bacteria's surface structure resulted in cell wall damage and their contents spilled over with the growth of the staining time. Some agglomerated cells with DOX adhered on surface or engulfed inside bacteria can emit strong fluorescence. It is evident that DOX can specially interact with the bacteria, manifested as a remarkable decrease in the number of fluorescent labeling cells.

Insight into the specific interaction sites could be readily obtained from Raman spectroscopy, in which vibration spectra can be acquired from the various depths within the colony.[28] As shown in Figures 4A and S3 and Table S1 (Supporting Information), the surface enhanced Raman spectroscopic (SERS) study of *E. coli* and *S. aureus* on the nanostructured Au NPs modified ITO electrodes demonstrates the specific binding behavior of the anthracycline antibiotic drug with target bacteria. Among the typical peaks of relevant bacteria, such as folding of the proteins, amino acids, DNA fragments (1125 cm^{-1}), single bases (A, G, T, and C), the important feature is the strong peak band at 1270 to 1325 cm^{-1}, which is typical of folded proteins separated to two closed peaks due to the pentose effect.[29,30] The deformations at 690 and 734 cm^{-1} are especially characteristic of adenine. The relevant peak intensity at 630 cm^{-1}, which may be attributed to the ring stretching of

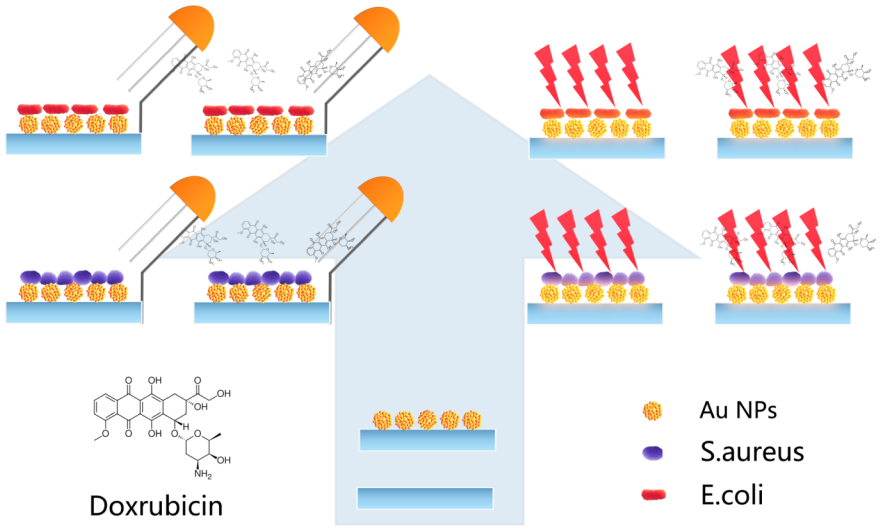

Figure 3. Schematic illustration for bacteria detection by using nanostructured Au based biosensor. In the first step, the nanostructured Au modified ITO electrode was prepared by the multipotential step technique. Then, a drop of 10 μL of cell suspension including *E. coli* or *S. aureus* is deposited onto the nanostructured Au modified electrode and placed in the incubator at 37 °C for 2 h. Afterward, a drop of 10 μL of DOX solution is added to the nanointerface of the nanostructured Au modified ITO electrode and detected through electrochemical study or Raman spectroscopy.

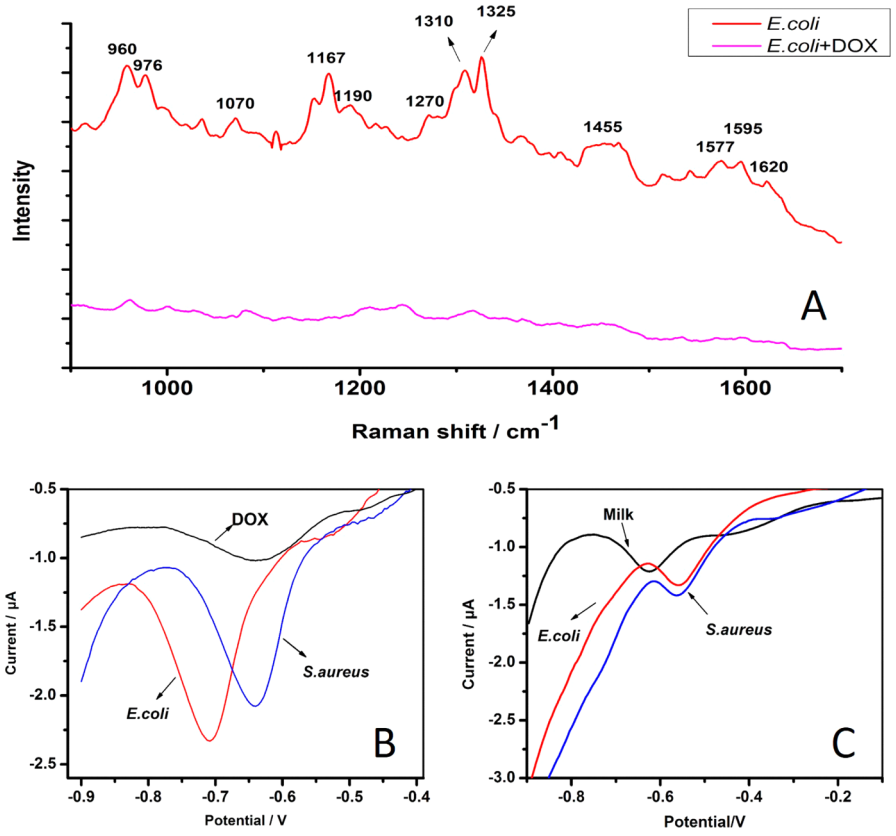

Figure 4. (A) Raman spectra of *E. coli* (top curve) and *E. coli*+DOX (0.5 mM) (bottom curve) on the nanostructured Au-coated ITO electrode. Excitation wavelength, 785 nm; laser power, 1 mW. (B) DPV study of DOX (0.5 mM) on the nanostructured Au-coated ITO in the absence (black color) and presence of *E. coli* bacteria (red) and *S. aureus* (blue). (C) DPV study of DOX (0.5 mM) on the nanostructured Au-coated ITO in pure milk (black color) and milk in the presence of *E. coli* (red color) and *S. aureus* (blue). Pulse amplitude, 0.05 V; pulse width, 0.05 V; pulse period, 0.1 s. The relevant DPV study could be completed in a few minutes.

phenylalanine, is found to sharply increase on the nanostructured Au modified ITO electrodes. Especially, vibrations close to the 960 and 977 cm^{-1} peaks are typically characteristic of denatured DNA, which are also separated by the pentose effect.[31−33] And the vibrations at 1577 and 1595 cm^{-1} are especially characteristic of A, T, and G, while the vibration around 1167 cm^{-1} is a typical stretching. Meanwhile, a slight increase of the peak intensity at 1680 cm^{-1} was also observed in the protein amide I regions (approximately 1670 cm^{-1}).[34,35] Vibrations at 535 and 1620 cm^{-1} are especially characteristic of

ν (S═S) and amide I. In addition, the vibration around 817 and 1070 cm^{-1} represent the peak of tyrosine and phenylalanine, respectively. Upon addition of the DOX, most peaks are observed to decrease, and some peaks are smeared out, as shown in Figures 4A and S3 (Supporting Information). It is noted that the typical peaks between 800 and 900 cm^{-1} disappear, which could be attributed to the relevant drug binding to the cell wall, and may considerably affect the structure and property of the cellular membrane.

3.3. Electrochemical Detection of Bacteria Based on the Nanostructured Au NPs Modified ITO Electrode. Based on the above observations, the Au NPs modified ITO electrode has been further utilized for the specific molecular recognition and electrochemical detection of relevant bacteria. As shown in Figure 4, our electrochemical study demonstrates the significant effect of the bacteria on electrochemical behavior of the drug molecules of DOX. It is observed that upon addition of *E. coli*, the peak current of DOX apparently increased, accompanying with the negative shift of 60 mV in the peak potential (Figure 4B). The significant difference of the electrochemical changes upon addition of bacteria could be attributed to the relevant biointeractions between this typical anthracycline antibiotic drug and target bacteria. Thus, the considerably different electrochemical behavior of DOX in the presence of different bacteria could be used to deduce the special binding behavior of the doxorubicin to related bacteria, which may readily afford different specific microenvironments for the target binding site. The sensor probes the attachment of bacterial cells by measuring the change in electrical properties of the molecular probe due to its different binding behavior with the cell membrane. Because biological cells consist of complex materials that have very different electrical properties, the presence of intact cell membranes on the electrodes significantly affects the electrochemical characteristics of the sensing signal. In the presence of a redox molecular probe, it can sensitively probe the changes of the biological events occurring on its surface/or inner by measuring the induced changes in faradaic impedance.

Moreover, electrochemical determination of bacteria on the Au NPs modified ITO electrodes could be further illustrated by using EIS, where the relevant behavior of the impedance biosensor system can be well evaluated by the Randles model equivalent circuit, as shown in Figure 5. The equivalent circuit consists of ohmic resistance (R_s) of the electrolyte, the polarization resistance (R_p) of the electrode, and the constant phase element (CPE).[36] The corresponding Nyquist plots of impedance spectra on bare ITO electrodes demonstrated that upon addition of *E. coli* on the bare ITO electrode, the charge transfer resistance (R_{ct}) values of $[Fe(CN)_6]^{3-/4-}$ significantly increased, indicating that the cell adhesion to the bare ITO electrode could significantly block the electron transfer of the electrochemical probe. Interestingly, it is noted that the relevant R_{ct} values remarkably decreased on the Au NPs modified ITO electrodes, and the related conductivity is excellent even in the presence of *E. coli*. The rational behind this could be attributed to the extraordinary electrochemical catalytic activity of the nanoporous Au film of the modified ITO electrodes to the oxidation of lipids on the microbial cell membrane. Upon addition of different concentration of *E. coli*, a linear relationship between the R_{ct} value and the log value of the concentration of cells could be obtained, where the fitted equation could be depicted as $R_{ct} = 24.45 \times \log CFU - 142.82$ ($R = 0.998$). The relative detection limit is 150 CFU/mL ($S/N = 3$).

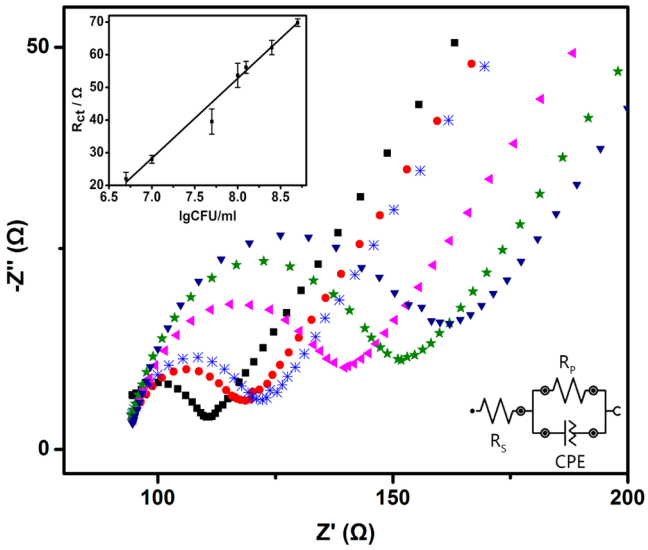

Figure 5. EIS study on the nanostructured Au coated ITO electrode covered with *E. coli*. The electrolyte is 5 mM $[Fe(CN)_6]^{3-/4-}$ containing 0.1 M KCl. Frequency range, 10^{-1}–10^5 Hz; amplitude, 5 mV. Bottom-right inset: the equivalent circuit, which is fitted by NOVA1.7. Top-left inset: the linear relationship curve between the R_{ct} values and the logarithm values of the *E. coli* concentrations ($R = 0.998$).

The relevant electrochemical strategy based on the nanostructured Au modified electrode could be readily utilized to detect or monitor some unexpected bacteria in real samples. For instance, the proposed assays have also been attempted in milk samples, as shown in Figure 4, when 0.5 mM DOX mixed in blank group (i.e., milk alone), a peak of DPV study appeared at −0.64 V. The relevant peak was observed to shift to −0.55 V upon addition of *E. coli* or *S. aureus*. And the relevant detection reproducibility in milk samples is satisfying, with an interbatch %DPV of less than 3%. On the basis of the apparent difference of the related current change and peak shift, we can directly and rapidly detect the polluted bacteria in milk. Thus, this new strategy of rapid bacteria detection could be further utilized for monitoring bacteria related pollution of food and other real samples for the efficient diagnosis of the multidrug-resistant bacteria or other disease related bacteria.

4. CONCLUSIONS

In this contribution, the rapid and ultrasensitive detection of some multidrug resistant bacteria like *E. coli* and *S. aureus* has been explored by SERS and electrochemical study. The results demonstrate that by using nanostructured Au NPs modified ITO electrodes, DOX can act as the sensitive probe to specifically recognize relevant bacteria and facilitate the rapid determination with high sensitivity. The real-time detection of multidrug resistant bacteria on the nanostructured Au modified ITO electrode could be readily realized in some real samples, which has been illustrated to be applicable for related bacteria detection in milk. This raises the possibility for the application of the established the nanostructured Au based electrochemical biosensors for rapid bacteria detection or monitoring of the relevant biological process in some complicated environments.

■ ASSOCIATED CONTENT

Supporting Information

Laser confocal fluorescence microscopy (LCFM) images and DPV and Raman spectroscopic study of the specific interaction of DOX with relevant bacteria on the nanostructured Au coated ITO electrode. This material is available free of charge via the Internet at http://pubs.acs.org.

■ AUTHOR INFORMATION

Corresponding Author

*X. Wang. Tel: 0086-25-83792177. E-mail: xuewang@seu.edu.cn.

Notes

The authors declare no competing financial interest.

■ ACKNOWLEDGMENTS

We gratefully acknowledge the support from National Key Basic Research Program (2010CB732404), National Natural Science Foundation of China (81325011, 21327902), National High Technology Research and Development Program of China (2012AA022703), and Suzhou Science & Technology Major Project (ZXY2012028).

■ REFERENCES

(1) Schito, G. C. Is Antimicrobial Resistance Also Subject to Globalization? *Clin. Microbiol. Infect.* **2002**, *8*, 1−8.

(2) Ma, P.; Dong, X. W.; Swadley, C. L.; Gupte, A.; Leggas, M.; Ledebur, H. C.; Mumper, R. J. Development of Idarubicin and Doxorubicin Solid Lipid Nanoparticles to Overcome Pgp-Mediated Multiple Drug Resistance in Leukemia. *J. Biomed. Nanotechnol.* **2009**, *5*, 151−161.

(3) Lu, Y. C.; Chuang, Y. S.; Chen, Y. Y.; Shu, A. C.; Hsu, H. Y.; Chang, H. Y.; Yew, T. R. Bacteria Detection Utilizing Electrical Conductivity. *Biosens. Bioelectron.* **2008**, *23*, 1856−1861.

(4) Shah, R. R.; Kaewgun, S.; Lee, B. I.; Tzeng, T. R. J. The Antibacterial Effects of Biphasic Brookite-Anatase Titanium Dioxide Nanoparticles on Multiple-Drug-Resistant Staphylococcus Aureus. *J. Biomed. Nanotechnol.* **2008**, *4*, 339−348.

(5) Burtscher, C.; Wuertz, S. Evaluation of the Use of PCR and Reverse Transcriptase PCR for Detection of Pathogenic Bacteria in Biosolids from Anaerobic Digestors and Aerobic Composters. *Appl. Environ. Microbiol.* **2003**, *69*, 4618−4627.

(6) Allen, M. J.; Edberg, S. C.; Reasoner, D. J. Heterotrophic Plate Count Bacteria - What is Their Significance in Drinking Water? *Int. J. Food Microbiol.* **2004**, *92*, 265−274.

(7) Dyck, E. V.; Ieven, M.; Pattyn, S.; Damme, L. V.; Laga, M. Detection of *Chlamydia Trachomatis* and *Neisseria Gonorrhoeae* by Enzyme Immunoassay, Culture, and Three Nucleic Acid Amplification Tests. *J. Clin. Microbiol.* **2001**, *39*, 1751−1756.

(8) Jokerst, J. C.; Emory, J. M.; Henry, C. S. Advances in Microfluidics for Environmental Analysis. *Analyst (Cambridge, U. K.)* **2012**, *137*, 24−34.

(9) Shepard, J. R. E. Polychromatic Microarrays: Simultaneous Multicolor Array Hybridization of Eight Samples. *Anal. Chem.* **2006**, *78*, 2478−2486.

(10) Xu, L. J.; Du, J. J.; Deng, Y.; He, N. Y. Electrochemical Detection of *E. coli* O157:H7 Using Porous Pseudo-Carbon Paste Electrode Modified with Carboxylic Multi-Walled Carbon Nanotubes, Glutaraldehyde and 3-Aminopropyltriethoxysilane. *J. Biomed. Nanotechnol.* **2012**, *8*, 1006−1011.

(11) Florent, J. C.; Monneret, C. Doxorubicin Conjugates for Selective Delivery to Tumors. *Top. Curr. Chem.* **2008**, *283*, 99−140.

(12) Sanvicens, N.; Pastells, C.; Pascual, N.; Marco, M. P. Nanoparticle-based Biosensors for Detection of Pathogenic Bacteria. *TrAC, Trends Anal. Chem.* **2009**, *28*, 1243−1252.

(13) Wang, Y. L.; Newell, B. B.; Irudayaraj, J. Folic Acid Protected Silver Nanocarriers for Targeted Drug Delivery. *J. Biomed. Nanotechnol.* **2012**, *8*, 751−759.

(14) Booser, D. J.; Hortobagyi, G. N. Anthracycline Antibiotics in Cancer-Therapy - Focus on Drug-Resistance. *Drugs* **1994**, *47*, 223−258.

(15) Elit, L.; Hirte, H. Novel Strategies for Systemic Treatment of Endometrial Cancer. *Expert Opin. Invest. Drugs* **2000**, *9*, 2831−2853.

(16) Rezaei, B.; Saghebdoust, M.; Sorkhe, A. M.; Majidi, N. Generation of A Doxorubicin Immunosensor Based on a Specific Monoclonal Antibody-Nanogold-Modified Electrode. *Electrochim. Acta* **2011**, *56*, 5702−5706.

(17) Mora, L.; Chumbimuni-Torres, K. Y.; Clawson, C.; Hernandez, L.; Zhang, L. F.; Wang, J. Real-Time Electrochemical Monitoring of Drug Release from Therapeutic Nanoparticles. *J. Controlled Release* **2009**, *140*, 69−73.

(18) Mazerski, J.; Martelli, S.; Borowski, E. The Geometry of Intercalation Complex of Antitumor Mitoxantrone and Ametantrone with DNA: Molecular Dynamics Simulations. *Acta Biochim. Polym.* **1998**, *45*, 1−11.

(19) Bailly, C.; Colson, P.; Houssier, C.; Houssin, R.; Mrani, D.; Gosselin, G.; Imbach, J. L.; Waring, M. J.; Lown, J. W.; Henichart, J. P. Binding-Properties and DNA Sequence-Specific Recognition of 2 Bithiazole-Linked Netropsin Hybrid Molecules. *Biochemistry* **1992**, *31*, 8349−8362.

(20) Li, N.; Ma, Y.; Yang, C.; Guo, L. P.; Yang, X. R. Interaction of Anticancer Drug Mitoxantrone with DNA Analyzed by Electrochemical and Spectroscopic Methods. *Biophys. Chem.* **2005**, *116*, 199−205.

(21) Molinierjumel, C.; Malfoy, B.; Reynaud, J. A.; Aubelsadron, G. Electrochemical Study of DNA-Anthracyclines Interaction. *Biochem. Biophys. Res. Commun.* **1978**, *84*, 441−449.

(22) Katz, E.; Willner, I. Integrated Nanoparticle−Biomolecule Hybrid Systems: Synthesis, Properties, and Applications. *Angew. Chem., Int. Ed.* **2004**, *43*, 6042−6108.

(23) Katz, E.; Shipway, A. N.; Willner, I. In *Nanoparticles—From Theory to Applications*; Schmid, G., Ed.; Wiley-VCH: Weinheim, Germany, 2003; pp 368−421.

(24) Lown, J. W.; Hanstock, C. C.; Bradley, R. D.; Scraba, D. G. Interactions of The Antitumor Agents Mitoxantrone and Bisantrene with Deoxyribonucleic Acids Studied by Electron-Microscopy. *Mol. Pharmacol.* **1984**, *25*, 178−184.

(25) Tian, H. X.; Zhuang, G. Q.; Ma, A. Z.; Jing, C. Y. Arsenic Interception by Cell Wall of Bacteria Observed with Surface-Enhanced Raman Scattering. *J. Microbiol. Meth.* **2012**, *89*, 153−158.

(26) Knauer, M.; Ivleva, N. P.; Liu, X. J.; Niessner, R.; Haisch, C. Surface-Enhanced Raman Scattering-based Label-Free Microarray Readout for the Detection of Microorganisms. *Anal. Chem.* **2010**, *82*, 2766−2772.

(27) Li, R.; Zhang, H.; Chen, Q. W.; Yan, N.; Wang, H. Improved Surface-Enhanced Raman Scattering on Micro-Scale Au Hollow Spheres: Synthesis and Application in Detecting Tetracycline. *Analyst* **2011**, *136*, 2527−2532.

(28) Majzner, K.; Kaczor, A.; Kachamakova-Trojanowska, N.; Fedorowicz, A.; Chlopicki, S.; Baranska, M. 3D Confocal Raman Imaging of Endothelial Cells and Vascular Wall: Perspectives in Analytical Spectroscopy of Biomedical Research. *Analyst* **2013**, *138*, 603−610.

(29) Wang, Y. L.; Lee, K.; Irudayaraj, J. Silver Nanosphere SERS Probes for Sensitive Identification of Pathogens. *J. Phys. Chem. C* **2010**, *114*, 16122−16128.

(30) Walter, A.; Marz, A.; Schumacher, W.; Rosch, P.; Popp, J. Towards a Fast, High Specific and Reliable Discrimination of Bacteria on Strain Level by Means of SERS in a Microfluidic Device. *Lab Chip* **2011**, *11*, 1013−1021.

(31) Chen, Q.; Lee, T.; Kumar, A. Y.; Min, J.; Choi, J. W. Analysis of Nanoscale Protein Film Consisting of Lactoferrin/11-MUA Bilayers for Bioelectronic Device. *J. Biomed. Nanotechnol.* **2013**, *9*, 849−855.

(32) Suh, J. S.; Moskovits, M. Surface-Enhanced Raman-Spectroscopy of Amino-Acids and Nucleotide Bases Adsorbed on Silver. *J. Am. Chem. Soc.* **1986**, *108*, 4711−4718.
(33) Efrima, S.; Zeiri, L. Understanding SERS of Bacteria. *J. Raman Spectrosc.* **2009**, *40*, 277−288.
(34) Knauer, M. N.; Ivleva, P.; Liu, X. J.; Niessner, R.; Haisch, C. Surface-Enhanced Raman Scattering-based Label-Free Microarray Readout for the Detection of Microorganisms. *Anal. Chem.* **2010**, *82*, 2766−2772.
(35) Kirschner, C.; Maquelin, K.; Pina, P.; Thi, N. A. N.; Choo-Smith, L. P.; Sockalingum, G. D.; Sandt, C.; Ami, D.; Orsini, F.; Doglia, S. M.; Allouch, P.; Mainfait, M.; Puppels, G. J.; Naumann, D. Classification and Identification of Enterococci: A Comparative Phenotypic, Genotypic, and Vibrational Spectroscopic Study. *J. Clin. Microbiol.* **2001**, *39*, 1763−1770.
(36) Wu, X. J.; Jiang, H.; Zhou, Y. Y.; Li, J. Y.; Wu, C. H.; Wu, C. Y.; Chen, B. A.; Wang, X. M. Selective Determination of Drug Resistant Cancer Cells on Indium Tin Oxide Electrode Modified with Nano Titanium Oioxide. *Electrochem. Commun.* **2010**, *12*, 962−965.